Block Nested Refinement and Numerical Estimation for Sudden Expansion Pipes in Various Step Angles

CHRISTINA G. GEORGANTOPOULOU
School of Engineering, Bahrain Polytechnic
Isa Town, Po box 33349
KINGDOM OF BAHRAIN
Christina@polytechnic.bh

Abstract: - The numerical simulation and estimation of flows inside channels is an essential tool for various applications due to the critical contribution in pipe control and inspection issues. In the present paper a simple, flexible and accurate numerical methodology is developed for the incompressible flows study inside sudden expansion pipes. Due to the nature of the physical domain the Cartesian grid approach is indicated for the domain discretization while it is combined with a block nested refinement technique in order to overcome the large number of computational cells are created due to the high aspect ratio of the specific problems. We develop testing of the refinement technique concerning the accuracy in various refinement factors as well as the step angle influence to the flow behavior and characteristics inside the pipe. The Navier-Stokes equations are solved using third accuracy upwind schemes in combination with the artificial compressibility technique for the pressure and the flux-vector splitting technique for the relating vectors. The flow behavior and variables are presented for various Reynolds numbers and step angle values in order to identify the optimum relation among expansion ratio, flow rate and separation zones. Corresponded results by the literature and by other numerical techniques are used for validation purposes presenting accepted convergence.

Key-words: - flow in pipes, sudden expansion, block nested grids, Navier-Stokes equations

1 Introduction

The incompressible flows inside pipes meet various applications in the industrial sector. Two are the most common geometrical particular characteristics in pipes except for their straight parts; the internal diameter variation and the junctions. The expansion channels are widely used for air, water, crude oil or gas flows and the elimination of energy losses and recirculation inside the flow remains the main engineering concern. In order to achieve it the numerical simulation estimation and control of flow is needed to be developed using simple and accurate models, easily adapted to certain common industrial flows.

Many other researchers have been involved in the above issue such Santos [1], where emphasis is given not only to the computational estimation of the flow but also to the experimental validation of the results. By the other hand Louda [2], has applied for the certain flow estimation a finite element method producing quite satisfied accuracy focusing at the recirculation zones' location [3]. Wallin [4], develops an explicit methodology and present flow variables results for high Reynolds (*Re*) numbers flows which is applied quite satisfactory for the sudden expansion channels flow simulation and computation, while more interesting numerical results have been produced in order to satisfy better flow behavior inside the pipes [5].

In all the above approaches, quite important flow information is presented but more focus is needed at the inclination angle effect to the developing flows in order to present useful conclusions and advices for industrial applications. Cartesian grids present better flexibility and support easy discretization of the governing equations if the geometry description allows to be applied. In the case of flows inside pipes Cartesian grids are appropriate ones in combination with an approximation technique in order to overcome the curvilinear pipe parts if these exist. Corrier [6] for example, has presented a quite flexible Cartesian grid scheme which can be independent by the geometrical bound and produces accurate flow results, while similar approaches develop techniques based approximated bounds creation using only grid lines in order to describe the flow domain [7]. Apparently, the uniform Cartesian grid generation cannot be satisfied when geometries with high aspect ratios are simulated. Interesting refinements techniques have been presented by Wang [8], where a quadrilateral grid generator is presented based on cell cutting or other adaptive techniques promise high accuracy with reduction of the computational memory simultaneously [9].

In the present paper a block nested refinement methodology is developed and tested for the incompressible flows inside sudden expansion pipes for a range of certain step angles. An additional main objective of this work is also the investigation and the specification of the relation among flow rate and separation zones, according to the step angles inside the pipe, in order to conclude to the best possible relationship between these and minimizing the energy loses of the flow simultaneously. The Cartesian grid methodology is developed using only grid lines, which can be applied for every channel geometry domain and the methodology is based on our previous research [10, 11]. The chosen refinement technique will be developed based on block nested sub-grids sequence at the crucial or curvilinear areas of the geometry for various values of the refinement factor and grid levels [12, 13]. It will be proved and presented that the above methodology is beneficial for the current flow cases and accurate, reducing the computational time simultaneously. The solution scheme for the Navier – Stokes equations is comprised of the flux vector splitting methodology in combination with the artificial compressibility technique [14], an accurate scheme which has been applied in various incompressible flow solutions in the past.

2 Numerical Model

The mathematical modeling is comprised of three main sections; the grid generation technique, the appropriate way of boundary conditions application and the numerical solution of the governing equations. However, due to the block nested refinement technique a special treatment is needed concerning the boundary conditions application according to the type of each bound and the location of each sub grid.

2.1 Geometry description and grid development

Concerning the numerical estimation of flows inside pipes, the Cartesian grids are more appropriate, although non - Cartesian bounds are met according to the channels' shape. At the flow case of the inclined step pipes, there is only one non-Cartesian bound, which is not enough to force the hybrid grids application as some of the researchers prefer [5] although the accuracy of the results is very satisfied. In our method all the geometry bounds are laid on Cartesian grid lines and consequently in order to succeed it we produce an approximated bound close as possible to the original one. The initial description of the geometry is achieved by a set of data points, which are used in combination with the rule of minimum distance in order to produce the new approximated data ones . All the new points are grid nodes and are connected with straight grid lines applying the saw-tooth method. For the case of pipes with inclined step, only one bound is non-Cartesian, which will be approximated using the above method. More details about this technique can be found in our previous research work [11, 15].

In order to face the high aspect ratios which are presented in all the pipes' structures, a refinement technique is necessary to be applied in order to reduce the computational time and memory and achieve the desired accuracy simultaneously. The refinement technique which has been chosen is a block nested methodology by the use of a hierarchical structured grid approach. The method is based on using a sequence of nested rectangular meshes in which numerical simulation is taking place (Fig. 1). The whole domain is a rectangle, whose sides lie in the coordinate directions, except for the case of the inclined step outer bound. At that domain location, only three edges are straight lines while the fourth one is a crooked one, due to the approximation technique. We simulate the domain creating as many refine grids as we need according to the flow domain demands [11].

The proposed nested algorithm contains several levels of grids. We name the coarsest level $l=0$ and each next refine sub – grid is named $l+1$. We define the integer refinement factor I, as follows:

$$I = dx_m / dx_{m+1} = dz_m / dz_{m+1}. \qquad (1)$$

where I is the refinement factor, dx_m *and* dx_{m+1} the grid's resolution in longitude for the m grid level and for the m+1 (next) grid level, respectively, while dz_m *and* dz_{m+1} the grid's resolution in latitude for the grid levels as above. The I is always a power of two while the choice of the location for the nested grids is usually according to the velocity differences at the adjacent cells.

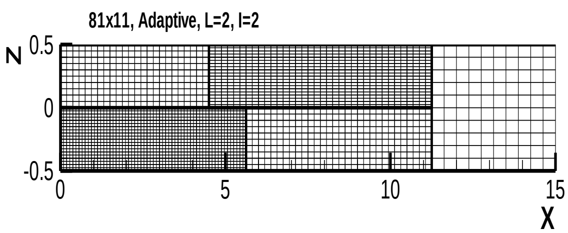

Fig. 1. Block nested grid refinement approach for a short pipe, based grid size: 81x11, two (2) levels of refinement, integer refinement factor equal to two (2).

2.2 Governing equations & numerical scheme

In order to numerical calculate the incompressible flow along the pipes we solve the system of the Navier – Stokes equations in combination with the mass conservation one. The N-S equations in Cartesian coordinates, two dimensional can be seen below:

$$\frac{\partial \rho}{\partial t} + \frac{\partial(\rho u)}{\partial x} + \frac{\partial(rw)}{\partial z} = 0 \qquad (2)$$

$$[\Gamma]\frac{\partial q}{\partial t} + \frac{\partial e}{\partial x} + \frac{\partial g}{\partial z} = \frac{1}{\mathrm{Re}}\left(\frac{\partial r}{\partial x} + \frac{\partial s}{\partial z}\right) \qquad (3)$$

$$[\Gamma]\frac{\partial q}{\partial t} + \frac{\partial e}{\partial x} + \frac{\partial g}{\partial z} + \alpha \cdot \frac{g_1}{z} = \frac{1}{\mathrm{Re}}\left(\frac{\partial r}{\partial x} + \frac{\partial s}{\partial z} + \alpha \cdot \frac{s_1}{z}\right) \qquad (4)$$

where,

$$[\Gamma] = \mathrm{diag}\left(\frac{1}{\beta},1,1\right)^T \qquad (5)$$

after the addition of the artificial compressibility term β, a is a switch for the activation of the axisymmetric terms ($\alpha=0$ is non axisymmetric, $a=1$ axisymmetric flow field), Re the Reynolds number and Q the unknown solution vector, $Q = (p \quad u \quad w)^T$, with p being the pressure, and (u, w) the velocity components in physical space. e, g, g_1 and r, s, s_1 are respectively the convective and diffusive flux vectors at the plane (x, z). The above N-S equations are the governing equations for unsteady flow but these can be used for steady flows, as in our case, using the time derivative for the iterative technique construction. These are also used for the solution of steady flow fields as in our case. In these steady cases the time derivative is used for the construction of an iterative technique using the artificial time step in order to define our final steady state [14].

2.3 Boundary conditions

The boundary conditions need a special treatment due to the block nested grid algorithm development. The conditions which are appropriate to be applied are related to the type of the interface that is met during the numerical solution of the flow equations.

The boundaries at the physical bounds are either Dirichlet either Neumann conditions according to the bound nature, as these can be seen at the below Table 1 with reference to Fig. 2, where u *and* w are the velocity components, p the pressure and the indicator *ref* shows the reference values of the field.

The method which is applied in our approach is a finite volume methodology which in the case of the 2-D Cartesian grids is almost similar with the finite difference one. According to the location of each bound backward or forward differences are applied in order to set the appropriate conditions. Similar approaches successfully have been developed in pipe simulation in our previous research work or even in numerical schemes with other various applications [16,17].

At the initial steps of the block nested algorithm, the velocity values will be transferred from a coarse interface (grid level $= l_i$) to a refine one (grid level $l = l_{i+1}$). It is important to be mentioned that in this stage the artificial (ghost) cells are neglected, while the velocity values are set as below:

$$u_{l,m} = u_{l,m+1} = u_{i,j} \qquad (6)$$

where $u_{l,m}$ and $u_{l,m+1}$ are the axial velocity components at the refined grid level and $u_{i,j}$ the corresponded one at the coarse level. The vertical velocity component is transferred by a similar way as follows:

$$w_{l,m} = w_{l,m+1} = w_{i,j} \qquad (7)$$

All the symbols are as these described above.

In the case that the boundary values must be transferred through fine – course interface the below formula is applied:

$$u_{i,j} = \frac{u_{l,m+1}+u_{l,m}}{2} \quad (8)$$

$$w_{i,j} = \frac{w_{l,m+1}+w_{l,m}}{2} \quad (9)$$

where the values are as described above.

Table 1: Boundary conditions for the inclined step pipe (Fig. 2)

Geometry Bounds (Fig. 2)	**Boundary Condition**
AB	Inlet conditions $u = u_{ref}$, $w=0, \frac{\partial p}{\partial x}=0$
AC	No slip condition (wall) $u=w=0, \frac{\partial p}{\partial z}=0$
CD	No slip condition (wall) $u=w=0, \frac{\partial p}{\partial z}=0$
DE	No slip condition (wall) $u=w=0, \frac{\partial p}{\partial z}=0$
EF	Outlet $\frac{\partial u}{\partial x}=0, w=0, p=p_{ref}$
BF	No slip condition (wall) $u=w=0, \frac{\partial p}{\partial z}=0$

In the case of fine-fine interfaces or course – course ones, similar philosophy is followed with the only difference that this time the values transferred as they are among sub-grids.

3 Results

In order to present accurate results and adequate evidence concerning the flow inside sudden expansion pipes the Cartesian block nested technique will be applied with the appropriate choice of sub-grids and refinement levels as well, trying to reduce the CPU time, reduce the computational memory and maintain the desired accuracy of our flow results. Consequently, validation data are presented in order to prove first of all the accuracy of the numerical scheme, as well as the efficiency of the block nested algorithm. By presenting the following analysis we attempt to enhance previous research work which has been done on the aforementioned flow fields [11] and extend our research work in incompressible viscous flows inside pipes [12,18].

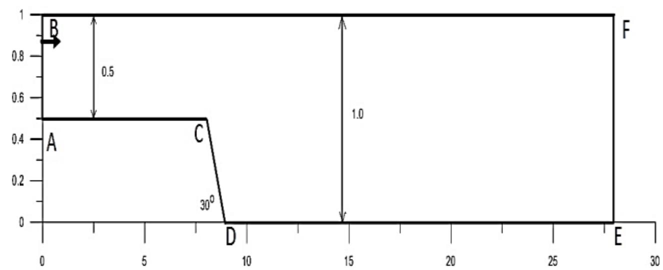

Fig. 2. Geometry description of the inclined step pipe. The dimensionless lengths of the channel vary according to the Re number value.

The geometry description and the related dimensions can be seen at the above Fig. 2. The relevant height H_{ref} has been set equal to 1 for dimensionless purposes.

We have studied, simulated and estimated various cases for four (4) different inclination angles values: 10^o, 30^o , 45^o and 90^o (Fig. 3), for five different Re numbers values: 100, 400, 800, 1200 and 1700. The numerical solution has taken place using uniforms and block nested grids with one or two levels of refinement in various mesh sizes, in order to prove the grid independence of the final solution.

The results that are presented have been produced using based grid size 351x26, with two refinement grid levels and refinement factor equal to two (2), I=2. In all the cases the expansion ratio is set to be equal to two (2). At the following Tables the separation zones of the lower and the upper wall of the pipes are presented according to the inlet flow rate for the above values of Re number. Detachment and reattachment points have been located in order to provide even more efficient information concerning the exact location of the separation zones for two different values of the step angle.

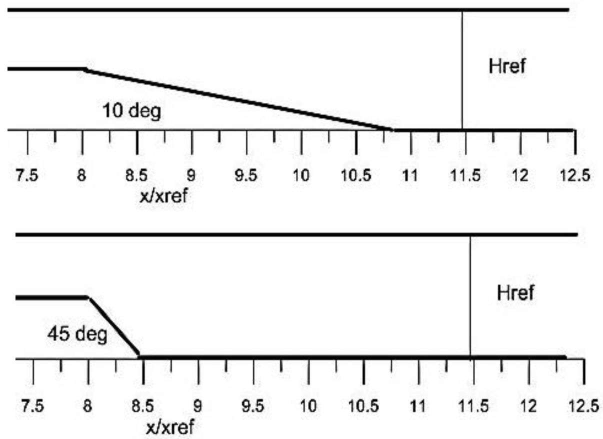

Fig.3. Part of the geometrical physical domains of the incline step pipe for two (2) values of the step angle.

Table 2: Recirculation zones lengths and related points: Lower Wall, inclination angle 10 deg. Block nested method, 351x13, l=2, I=2.

Re	**Lower Wall**		
	Recirculation Length	**Detachment Point**	**Reattachment Point**
100	No detection	No detection	No detection
400	No detection	No detection	No detection
800	No detection	No detection	No detection
1200	4.53	17.47	22.00
1700	8.07	18.71	26.78

Table 3: Recirculation zones lengths and related points: Upper wall, inclination angle 10 deg. Block nested method, 351x13, l=2, I=2.

Re	**Upper Wall**		
	Recirculation Length	**Detachment Point**	**Reattachment Point**
100	No detection	No detection	No detection
400	No detection	No detection	No detection
800	4.57	8.85	16.34
1200	7.54	8.53	18.71
1700	10.28	8.48	19.68

For validation purposes all the numerical cases solved using the commercial software ANSYS and some of these are presented for inclination angle equal to 30 deg for all the range of the used Re numbers, using uniform grid sized 651x26 (Tables 6 and 7). Additionally, in order to validate and check the efficiency and accuracy of the block nested algorithm similar numerical solutions for the flow variables have been produced using 651x26 Cartesian uniform grid (which is taken as the exact solution) as well as similar block nested grid with only one level of sub-grids. The convergence is satisfied enough, while the errors are low and acceptable concerning numerical schemes convergence and validation.

Table 4: Recirculation zones lengths and related points: Lower wall, inclination angle 30 deg. Block nested method, 351x13, l=2, I=2.

Re	**Lower Wall**		
	Recirculation Length	**Detachment Point**	**Reattachment Point**
100	0.39	8.90	9.29
400	4.15	8.26	12.41
800	6.46	8.26	14.72
1200	7.56	8.26	15.91
1700	8.94	8.26	17.20

Table 5: Recirculation zones lengths and related points: Upper wall, inclination angle 30 deg. Block nested method, 351x13, l=2, I=2.

Re	**Upper Wall**		
	Recirculation Length	**Detachment Point**	**Reattachme nt Point**
100	No detection	No detection	No detection
400	No detection	No detection	No detection
800	4.74	13.54	18.28
1200	7.54	14.51	22.05
1700	10.07	15.85	25.92

As it is depicted by all the Tables, there are mainly two separation zones the most, inside the channel, while the recirculation at the upper wall cannot be detected at Re numbers equal to 100 and 400 in most of the cases. As the flow rate increases, the recirculation length increases as well as on both of the channel's walls. However, although the detachment points at the lower wall remains at the same position for all the inlet velocities (around 8.26 except for the case of Re=100), the one at the upper wall is moving forward according to the related Re number. Despite of this fact the recirculation length at the upper bound is increased as the Re increases. At Tables 4 and 5 the related information is presented for inclination angle value equal to 30 deg. The numerical estimation has been developed using both of the computational techniques (block – Cartesian and ANSYS) for validation purposes, where the convergence of the results is very satisfied, presenting very low relative error ($4 \times 10^{-3} < rel.error < 5.5 \times 10^{-3}$).

Table 6: Recirculation zones lengths and related points: Inclination angle 30 deg. ANSYS – Fluent, Cartesian uniform grid 651x26.

Re	**Lower Wall**		
	Recirculation Length	**Detachment Point**	**Reattachment Point**
100	0.44	8.89	9.33
400	4.28	8.28	12.56
800	6.58	8.28	14.86
1200	7.74	8.28	16.02
1700	9.03	8.28	17.31

Table 7: Recirculation zones lengths and related points: Inclination angle 30 deg. ANSYS – Fluent, Cartesian uniform grid 651x26.

Re	**Upper Wall**		
	Recirculation Length	**Detachment Point**	**Reattachment Point**
100	No detection	No detection	No detection
400	No detection	No detection	No detection
800	5.02	13.55	18.57
1200	7.72	14.55	22.27
1700	10.13	15.93	26.06

Similar effects are depicted for all the other step angles. The main findings by the above Tables are that as you increase the flow rate, the expansion of the separation zones is increased as well. No detection of recirculation is presented in very low Re numbers while the appearance of the upper bound recirculation depends on the Re values and the inclination angle as well (Fig. 4). The influence of the inclination angle is very clearly presented, showing that as you increase the value of the angle more recirculation length is expected according to the Re number although the behavior of the fluids at the lower and at the upper wall is not the same.

Through Fig. 6, the influence of the Re number to the recirculation expansion is depicted for two values of the inclination angle. It seems that as more you increase the Re as more the recirculation is developed for both of the pipes walls. Exactly the similar findings are concluded for all the other values of the inclination angle.

Concerning the numerical procedure and the computational solution that it has been applied, it worth to be mentioned that the CFL number is possible to receive high values for Re numbers less than 1200. At the case of Re equal to 1700, many oscillations are appeared to the flow field if the CFL remains at high levels. Additionally in these cases the CPU time is huge sometimes or in some other cases no convergence of the flow field can be achieved.

It is recommended for Re numbers higher to 1300, the CFL to be less than 10, in order to achieve a stable and robust solution although in some cases the CPU time is much higher than was expected.

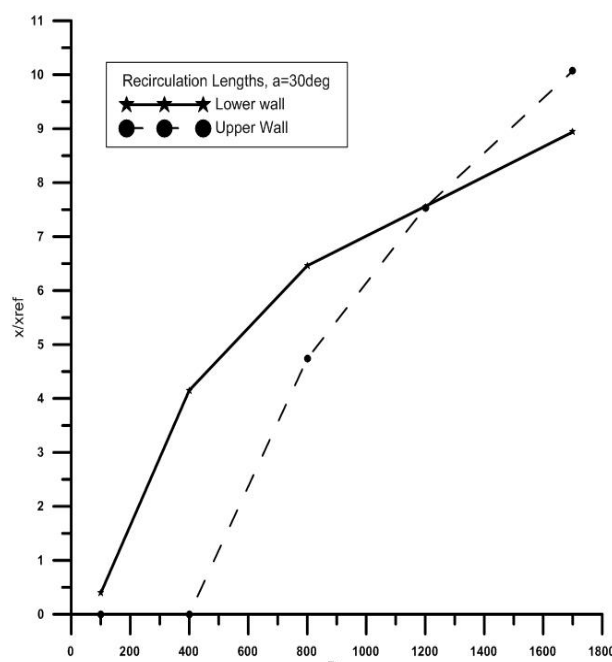

Fig. 4. Recirculation length variation according to the Re number.

Table 8: Computational cells and CPU time for grid types and sizes; inclination angle a=30 deg.

Inclination angle a=30 deg		
Grid type and size	**No of cells**	**CPU time**
Re=400		
Uniform 651x26	14,980	531.24
Block Nested 321x13 *I*=2, *l*=1	4,849	190.00
Block nested 321x13 *I*=2, *l*=2	10,078	223.65
Re=800		
Uniform 651x26	14,980	518.00
Block Nested 321x13 *I*=2, *l*=1	4,849	205.15
Block nested 161x13 *I*=2, *l*=2	10,078	237.49
Re=1700		
Uniform 651x26	14,980	1067.72
Block Nested 321x13 *I*=2, *l*=1	4,849	426.48
Block nested 161x13 *I*=2, *l*=2	10,078	527.15

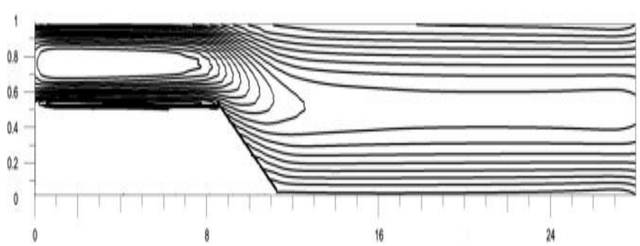

Fig.5. Velocity contours along the pipe. Block nested grid, *I=2, l=2*. Inclination angle equal to 10^o and *Re=100*. No recirculation zone is detected.

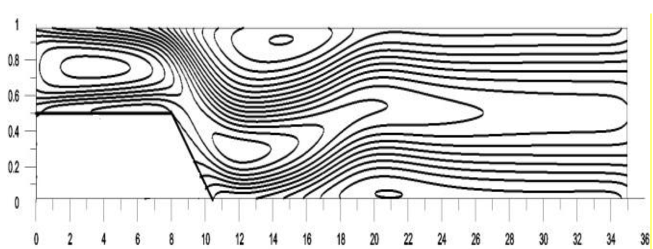

Fig. 6. Velocity contours along the pipe. Block nested grid, *I=2, l=2*. Inclination angle equal to 10^o and *Re=1200.* Very clearly are depicted upper and lower wall separation zones.

Although a first validation attempt of our numerical method has been achieved through Tables 3-4 and 6-7, further investigation is needed in order to check the efficiency of the proposed block nested algorithm to the aforementioned cases.

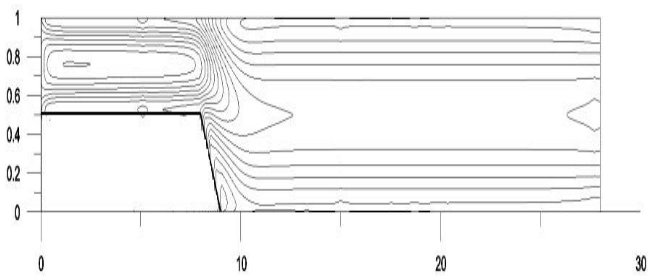

Fig. 7. Velocity contours along the pipe. Block nested grid, *I=2, l=2.* Inclination angle equal to 30^o and *Re=100.* It can be seen the small recirculation zone at the lower wall near to the inclined bound.

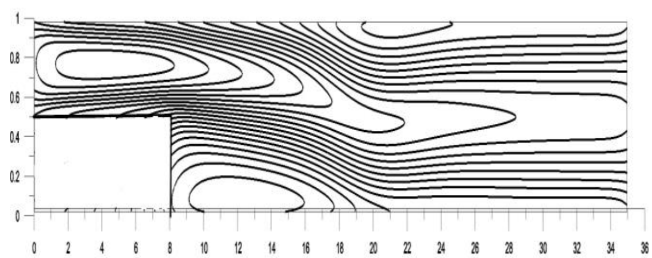

Fig. 8. Velocity contours along the pipe. Block nested grid, *I=2, l=2*. Inclination angle equal to 90^o and *Re=1200*. Very clearly are depicted upper and lower wall separation zones.

For these purposes the computational estimation of the flow has been developed using various types of Cartesian grids, uniform and block nested ones with one (1) and two (2) levels of refinement. In the Tables 8 the used computational cells and the corresponded CPU time are presented for different used grid types. By these data it seems that using the block nested grid approach the CPU time is reduced significantly in some cases, more than 65%, without losing concerning the accuracy of the results.

In order to set a more accurate image of the developing recirculation zones obtaining more details than the lengths and the related points, we present the following velocity contours for various values of inclination angles as well as Re numbers (Fig. 5-8). At Fig. 5 and Fig. 6 the flow distribution is presented when the angle *(a)* is equal to 10 deg, with no recirculation for *Re=100* and extended upper wall separation for *Re=1200*. At Fig. 7 the velocity contours are presented for angle *(a)* equal to 30 deg where the separation zones are varied according to the *Re* number value without any un-expectancy. The velocity contours for angle equal to 90 deg is finally presented (Fig. 8), providing certain details not only about the separation zones lengths but also for the related widths.

4 Conclusions

The behavior of the incompressible viscous flows inside sudden expansion pipes is presented to the present paper with details. The flow characteristics, variables distribution and certain data information as points of upper and lower bound separation zones have been analytically presented for various values of Re number. For the physical domain discretization we use Cartesian grids and we also develop a block nested refinement algorithm, which can be easily applied to the aforementioned flow domain. The artificial compressibility method has been applied for the numerical solution of the Navier-Stokes equations, while the appropriate way of the boundary conditions application has been studied according to each bound of the final discretized domain. It seems that if the Re number is higher than 400 two separation zones are developed inside the pipe in both of the bounds. The related detachment and reattachment points are clearly presented for every case and the final results show that in most of the cases the higher Re numbers the more extended recirculation for a certain inclination angle. In addition, as the pipe's inclination angle is increased, it seems that the recirculation length at the lower wall is increased as well, for all the range of Re number values. It worth to be mentioned, that this conclusion has been validated for all the range of Re numbers, using our proposed numerical technique, for various grid sizes uniform and ununiformed as well, either the corresponded one by ANSYS. By the above results, it seems that the accuracy of block nested algorithm is accepted. Further research will be developed in order to study also the influence of the expansion ratio in similar pipes.

References

[1] Lee T. and Mateescu D. Experimental and numerical investigation of 2-D backward-facing step flow. Journal of fluids and structures, vol. 12, pp. 703–716, 1998

[2] Louda P., Prihoda J.,Kozel K.,Svacek P., “Numerical simulations of flows over 2D and 3D backward facing inclined steps”, Int. Journal of heat and Fluid flow

[3] Torres Maj., Garcia J., Numerical characterization of particle dispersion in the turbulent recirculation zones of sudden expansion pipe flows, Proceedings of the 6th European conference on computational Fluid dynamics, Barcelona, 2014

[4] Wallin S., Johansson A.V., “ A complete explicit algebraic Reynolds stress model for incompressible and compressible turbulent flows”, Journal Fluid Mechanics, vol. 403, pp.89-132

[5] Shamloo H., Pirzadeh B., “Investigation of characteristics of separation zones in T-junctions”, Proc. Of Int. conference WSEAS on Water resources, Hydraulics and Hydrology, pp. 157-161, UK

[6] Coirier, W.J. and Powell, K.G., “An accuracy assessment of Cartesian-mesh approaches for the Euler equations”, J. of Computational Physics, Vol. 117, pp. 121-131, 1995

[7] Georgantopoulou Chr.G., Pappou Th.J., Tsaggaris S.G., “Cartesian grid generator for N-S numerical simulation of flow fields in curvilinear geometries”, Proceedings of the 4th GRACM congress on comput. Mechanics, pp. 526-534, 2002

[8] Wang, Z.J., “A Quadtree-based adaptive Cartesian/Quad grid flow solver for Navier-Stokes equation”, Computers and Fluids, Vol. 27, pp.529-549, 1998

[9] Iqbal S., Ansari A., Javed A., Siddiqui, “An adaptive Finite Element formulation for the solution of second order obstacle problems using quadratic lagrance polynomials”, Journal of Numerical Analysis, industrial and applied Mathematics, vol.9-10, pp.37-45, 2016

[10] Georgantopoulou C., Georgantopoulos G., Vasilikos N., Numerical analysis and modeling of recirculating flows, Int. Journal of mathematical Models and Method in Applied Sciences, 9 (2015) 248-260.

[11] Georgantopoulou C., Georgantopoulos G., Vasilikos N., Saw tooth approximation and numerical solution for flow in inclined channels, WSEAS Transactions on Fluid mechanics, 10 (2015) 69-79

[12] Chr.G. Georgantopoulou and S. Tsangaris, "Block mesh refinement for incompressible flows in curvilinear domains", Applied Mathematical Modeling,Vol.31, pp2136-2148.

[13] Berger M.J. and Collela P., "Local adaptive mesh refinement for shock hydrodynamics", J. of Comput. Physics, Vol. 83, pp.64-84, 1989.

[14] Pappou, Th. and Tsangaris, S., "Development of an artificial compressibility methodology using Flux Vector Splitting", International J. for Numerical Methods in Fluid, Vol. 25, pp.523-545, 1997

[15] Georgantopoulou Chr., Georgantopoulos G., Vasilikos N. and Tsangaris S., "Cartesian refinement grid generation and numerical calculation of flows around Naca0012 airfoil" Proceedings of Int. Conference on Applied mathematics, simulation, modeling, pp. 256-263.

[16] Mavromatidis, L., El Mankibi, M., Michel, P., Bykalyuk, A., & Santamouris, M. (2012). Guidelines to study numerically and experimentally reflective insulation systems as applied to buildings. Advances in Building Energy Research, 6, 2–35

[17] Mavromatidis, L., Michel, P., El Mankibi, M., & Santamouris, M. (2010). Study on Transient heat transfer through multilayer thermal insulation: Numerical analysis and experimental investigation. Building Simulation, 3, 279–294

[18] C. Georgantopoulou, Feras Ali, N. Vasilikos, G. Georgantopoulos, "Numerical modelling and investigation of crude oil flow in T-junction channels", Applied Mechanics and Materials, vol. 829, pp. 15-20, doi: 10.4028/www.scientific.net/AMM.829.15, 2016.